Progress In Electromagnetics Research Letters, Vol. 100, 27–34, 2021

Broadband Surface-Mount Dipole Antenna Array Using Highly Isolated Via Fence for 5G Millimeter-Wave Applications

Xiubo Liu[1], Wei Zhang[1], Dongning Hao[1], and Yanyan Liu[2, *]

Abstract—This letter proposes a 2×2 surface-mount dipole antenna array based on via fence for 5G millimeter-wave applications. The dipole antenna element was first proposed, which has a compact size and low cost. Then via fences are introduced to reduce the coupling between adjacent elements and enhance isolation. In this way, compared with a 1×2 antenna array without the via fence, the isolation of a 1×2 antenna array with a via fence is improved by 12 dB at 26 GHz. The elements are extended into 2×2 arrays with and without the via fence, and their performance is evaluated by the evaluation board. The measurement results show that the -10-dB impedance bandwidth of the antenna array is 19% (24.7–29.9 GHz), and the peak gain is 9.5 dBi at 25 GHz. The proposed 2×2 array can be used in the N257 (26.5–29.5 GHz), N258 (24.25–27.5 GHz), and N261 (27.5–28.35 GHz) frequency bands. Low cost, small size, and high isolation characteristics make it one of the candidates for 5G millimeter-wave applications.

1. INTRODUCTION

The millimeter-wave frequency band provides high carrier frequency and massive bandwidth to solve the shortage of global cellular communication for next-generation 5G applications. On the other hand, the atmosphere, rain absorption, and path loss in the millimeter-wave frequency band are stronger than those in the low-frequency band [1, 2]. To solve this problem, it is necessary to use an antenna array with an unprecedented number of antennas, which results in a smaller distance between the antenna elements. The smaller the distance is, the stronger the coupling is between the antennas. Strong coupling reduces the signal quality. Therefore, reducing the mutual coupling of antenna elements is one of the challenges for 5G millimeter-wave antenna arrays.

Many methods have been studied to suppress the coupling between antenna elements. The main methods are divided into the following categories, such as metasurface or metamaterial absorber [3, 4], electromagnetic bandgap structures (EBG) [5–9], metal strip resonators [10–13], and decoupling feeding network [14–16]. However, the above-mentioned methods have a large volume and a complicated structure. They are not suitable for the integration of 5G millimeter-wave systems. Via fence is a method to improve isolation and suppress the coupling between antenna and RF chip [17]. Capacitive via fences have been successfully verified to enhance the isolation of dual-polarized microstrip antennas while maintaining miniaturization and high port isolation [18].

Therefore, in this letter, we propose a solution based on the via fence to enhance the isolation of adjacent elements for the 28 GHz millimeter-wave antenna array. The prototype is designed on a low-cost single-layer FR4 substrate with two rows of via fences to enhance the isolation of the antenna elements. By using the BGA packaging, the prototypes have surface mount characteristics, which are more convenient to be integrated into the system. To verify the design, a 2×2 array prototype was fabricated and measured. The measured results are in good agreement with the simulated ones.

Received 17 July 2021, Accepted 13 September 2021, Scheduled 18 September 2021

* Corresponding author: Yanyan Liu (lyytianjin@nankai.edu.cn).

[1] School of Microelectronics, Tianjin University, Tianjin 300072, China. [2] Tianjin Key Laboratory of Photo-electronic Thin Film Devices and Technology, Nankai University, Tianjin 300071, China.

2. ANTENNA DESIGN

2.1. Antenna Element Configurations

Figure 1 shows the evolution of the antenna elements. First, it is derived from a planar two-dimensional (2D) endfire dipole antenna, as shown in Figure 1(a). The planar radiating dipole is fed by a grounded coplanar waveguide (GCPW). Secondly, Figure 1(b) shows a three-dimensional (3D) structure based on the 2D endfire antenna. With the help of plated through holes (PTH), the antenna feeds the dipole from the bottom feed point. Finally, the solder balls are installed at the bottom of the antenna to achieve the BGA packaging, as shown in Figure 1(c). The BGA packaging makes the antenna smaller and easier to integrate.

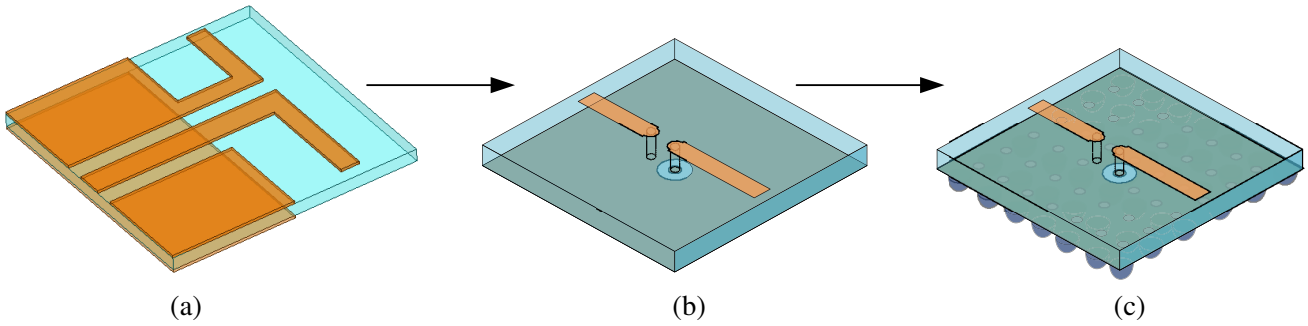

Figure 1. Design evolution of the proposed antenna element. (a) 2D planar endfire antenna. (b) 3D broadside antenna. (c) BGA packaged 3D broadside antenna.

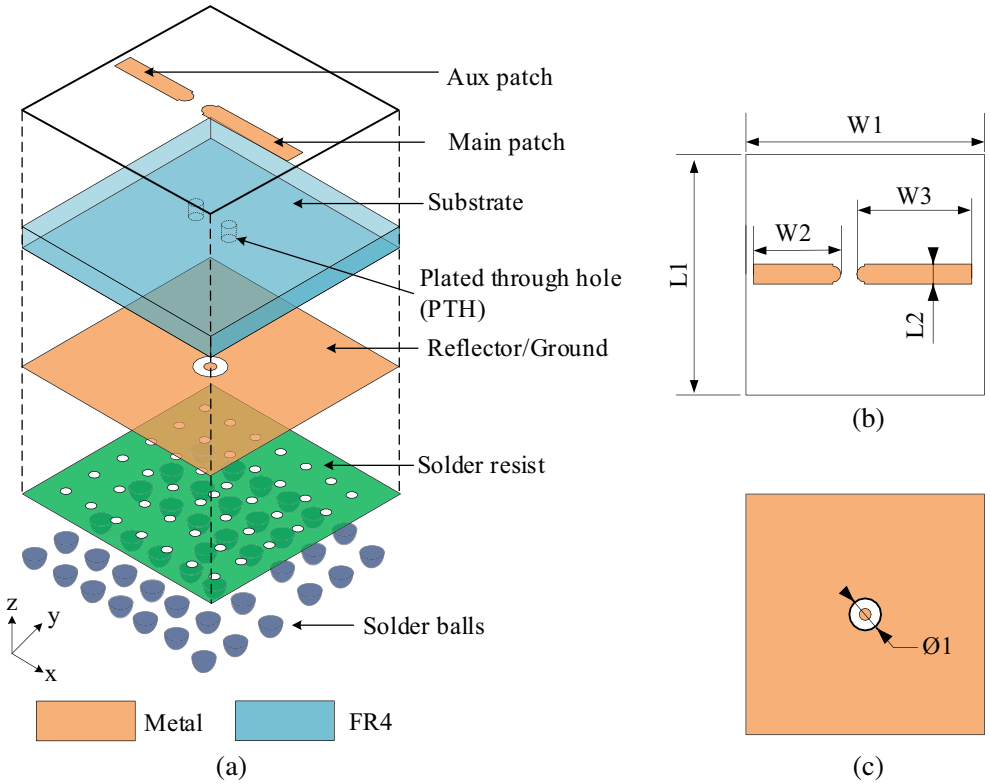

Figure 2. Geometry of the proposed antenna element. (a) Explored view. (b) Top view. (c) Bottom view.

The proposed antenna element is shown in Figure 2. The antenna consists of a single dielectric layer. It is manufactured on an FR4 substrate ($\varepsilon_r = 4.4$, $\tan\delta = 0.02$) with a thickness of 1.4 mm. The top layer of the antenna consists of two dipole patches. As shown in Figure 2(b), one is the main patch, and the other is the auxiliary patch. The main patch is connected to the bottom-feed point through PTH, and the auxiliary patch is directly connected to the bottom ground plane through another PTH. The bottom layer is mainly composed of the bottom feed point and ground plane. As shown in Figure 2(c), the feed point and ground plane are separated by an annular air gap. After optimization in the Ansys HFSS, the detailed dimensions of the proposed antenna element are given in Table 1. As shown in Figure 3, it can be observed that the simulation results show that in the 24–32 GHz frequency band, the antenna gain is 4.68–5.29 dBi, and the efficiency is between 88.7 and 91.09%.

Table 1. Dimensions of the proposed antenna element (units: mm).

Parameters	Values	Parameters	Values
$L1$	6	$W2$	2.2
$L2$	0.5	$W3$	2.9
$W1$	6	$\Phi1$	0.8

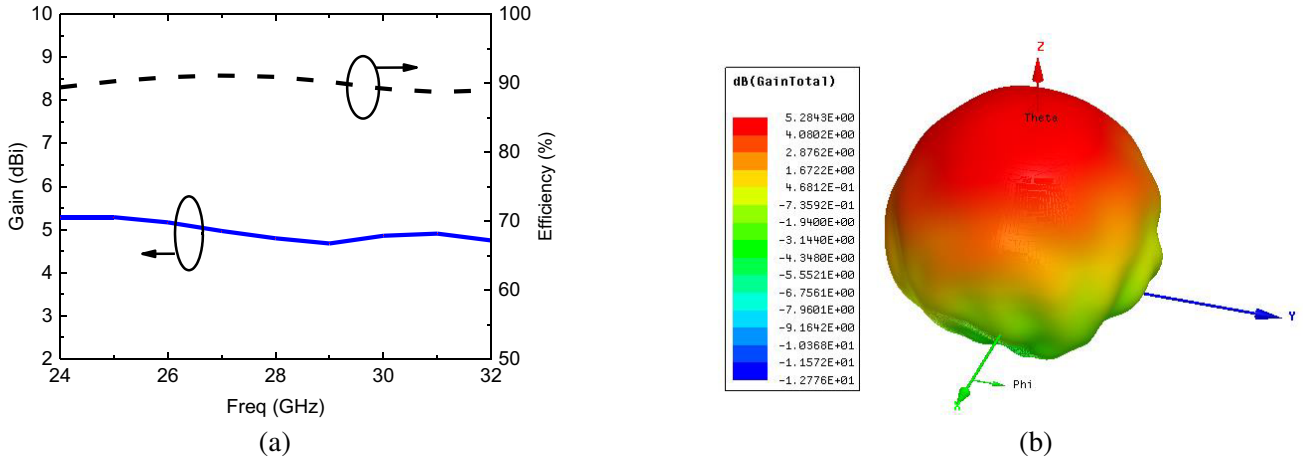

Figure 3. (a) Simulated gain and efficiency of the antenna element. (b) 3D radiation pattern at 28 GHz.

2.2. Adjacent Element Isolation

The 1×2 antenna array is shown in Figure 4. Based on the antenna element, a 1×2 antenna array with a size of 7 mm $\times$ 6 mm $\times$ 0.254 mm was made to evaluate the isolation. In Figure 4(b), a row of ground via fences is added based on Figure 4(a). The via fence can be equivalent to the electrical boundary and effectively shielding the electric field between the antenna elements, thereby improving the isolation between adjacent elements.

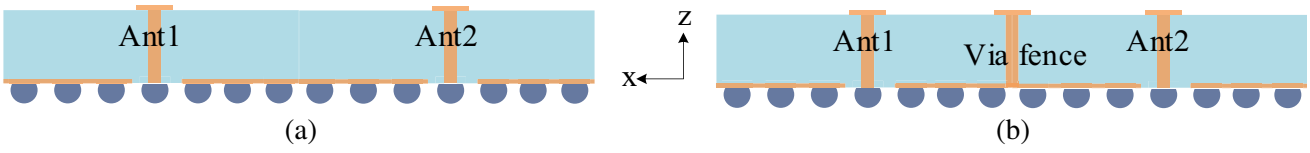

Figure 4. Cross-section of the proposed 1×2 antenna array (a) Without via fence. (b) With via fence.

Photographs of the 1×2 antenna array with and without the via fences are shown in Figures 5(a) and (b), respectively. The prototypes are mounted on the RO4350B evaluation board ($\varepsilon_r = 3.66$, $\tan\delta = 0.004$) with a size of 14 mm × 43 mm × 0.254 mm. The measurement results of port-to-port isolation are shown in Figure 5(c). It can be seen that the isolation of prototype without via fence is under −24.57 dB, while the isolation of prototype with via fence is under −27 dB. In particular, the isolation is −36.7 dB at 26 GHz, which is 12.1 dB higher than the prototype without via fence.

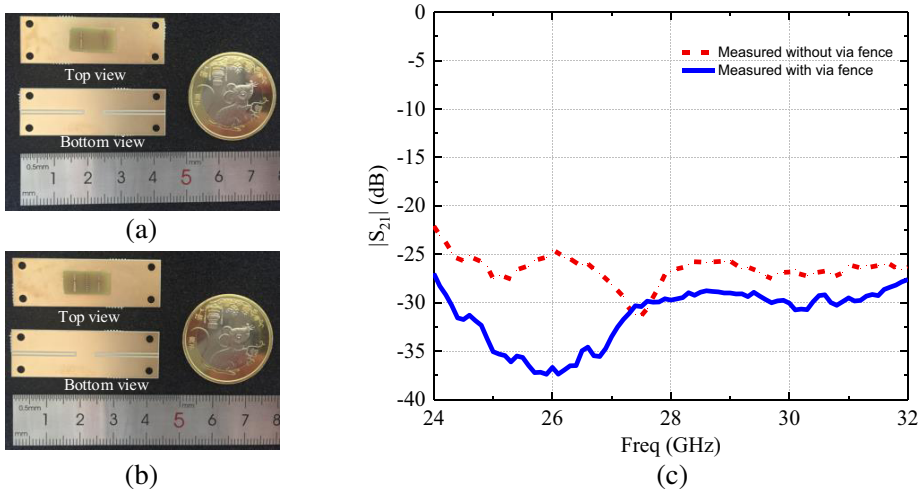

Figure 5. Photograph of the 1×2 antenna prototype. (a) Without via fence. (b) With via fence. (c) Measured S-parameters.

3. MEASUREMENT RESULTS AND DISCUSSION

Based on the above analysis, a 2×2 antenna array was made to verify the design. Figures 6(a) and (b) show photos of the prototypes with and without the via fence, respectively. The size of the 2×2 antenna array is 13 mm × 13 mm, and the center-to-center distance between adjacent elements is 7 mm. Similarly, as shown in Figures 6(c) and (d), the evaluation board is also made on the RO4350B board with a size of 28 mm × 34 mm × 0.254 mm. Three GCPW-based power dividers with one to two T-junctions converting the RF signal into four signals with the same amplitude and phase. Additionally, the width of the 50 Ω GCPW is 0.54 mm, and the width of the 35.35 Ω T-junction is 1.14 mm. After the prototypes are mounted on the evaluation board, the 2.92 mm connector is used to connect the evaluation board to the coaxial cable of the network analyzer (Rohde & Schwarz, ZVA40). Besides, the radiation patterns are measured in an anechoic chamber.

As can be seen from Figure 7(a), the −10 dB bandwidths of 2×2 prototypes with and without via fences are 24.7–29.9 GHz and 24.9–29.5 GHz, respectively. The bandwidth of the prototype with the via fence is slightly wider. The −10 dB impedance bandwidth covers the 5G millimeter-wave N257 (26.5–29.5 GHz and N261 (27.5–28.35 GHz) bands. As shown in Figure 7(b), the measured gains of the prototypes with and without the via fence are 8.3–9.5 dBi and 8.3–10.2 dBi in the range of 24.7 to 29.9 GHz. As can be observed in Figure 8, the measured and simulated normalization radiation patterns with and without the via fence are shown at 26, 28, and 30 GHz, respectively. Some discrepancies can be observed between the simulated and measured results, but an acceptable consistency is obtained due to the influence of manufacturing tolerance and measurement deviation. In the broadside direction, the measured E-plane cross-polarization of the prototype without the via fence is less than −21.2 dB, −25 dB, and −15.5 dB at 26, 28, and 30 GHz, respectively. Additionally, the measured cross-polarization of the prototype with the via fence is lower than −20.6, −18.8, and −19.4 dB, respectively. The via fence suppresses the cross-polarization level, especially at the high-frequency bands.

Table 2 shows a comparison with other reported work. Reference [18] also uses the via fence method, but it is used for the dual-Polarized ports inside the microstrip antenna. In this work, the via fence

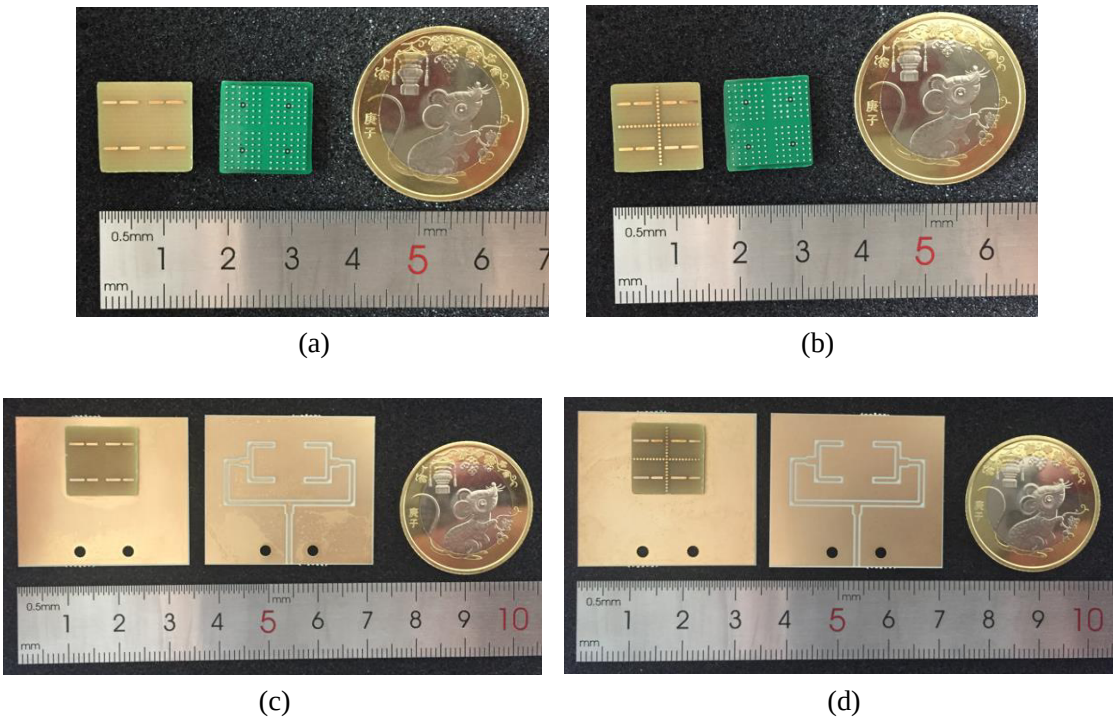

Figure 6. Photograph of the 2 × 2 array prototype. (a) Without via fence. (b) With via fence. Assembly prototype. (c) Without via fence. (d) With via fence.

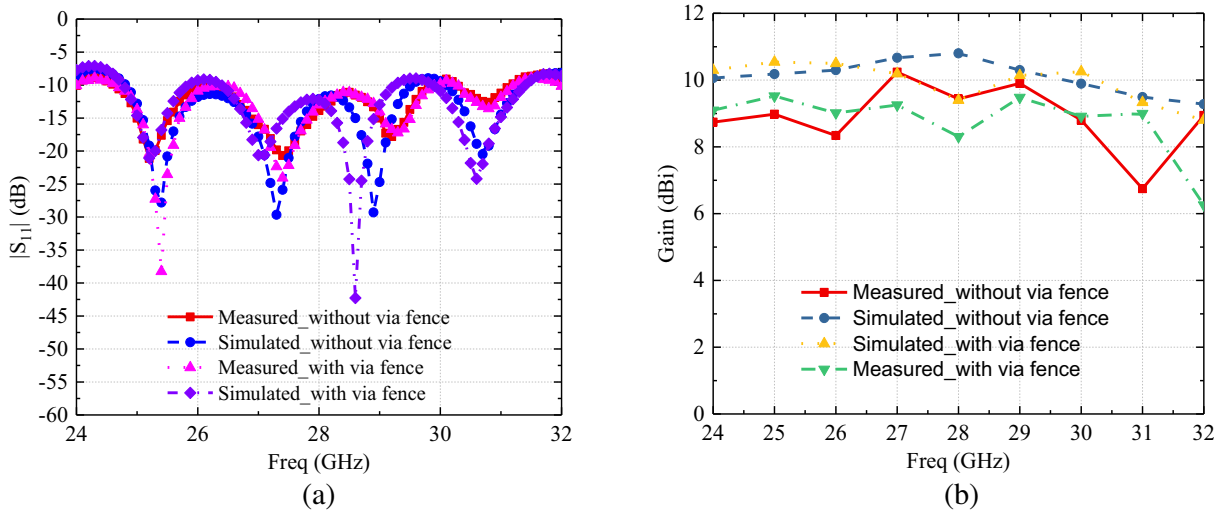

Figure 7. (a) Measured and simulated reflection coefficient of the prototype. (b) Measured and simulated peak gain of the prototype.

is used to enhance the isolation of the adjacent antenna element in the antenna array. Reference [14] realizes the optimal isolation between the adjacent elements, but the design of the decoupling network is relatively complex. Compared with [3] and [5], the proposed method achieves better impedance bandwidth, isolation, and antenna gain. The via fence also shows an effective way to enhance the isolation and suppress the coupling between adjacent antenna elements. Besides, the BGA packaging also makes the proposed antenna more suitable for integration in a millimeter-wave system.

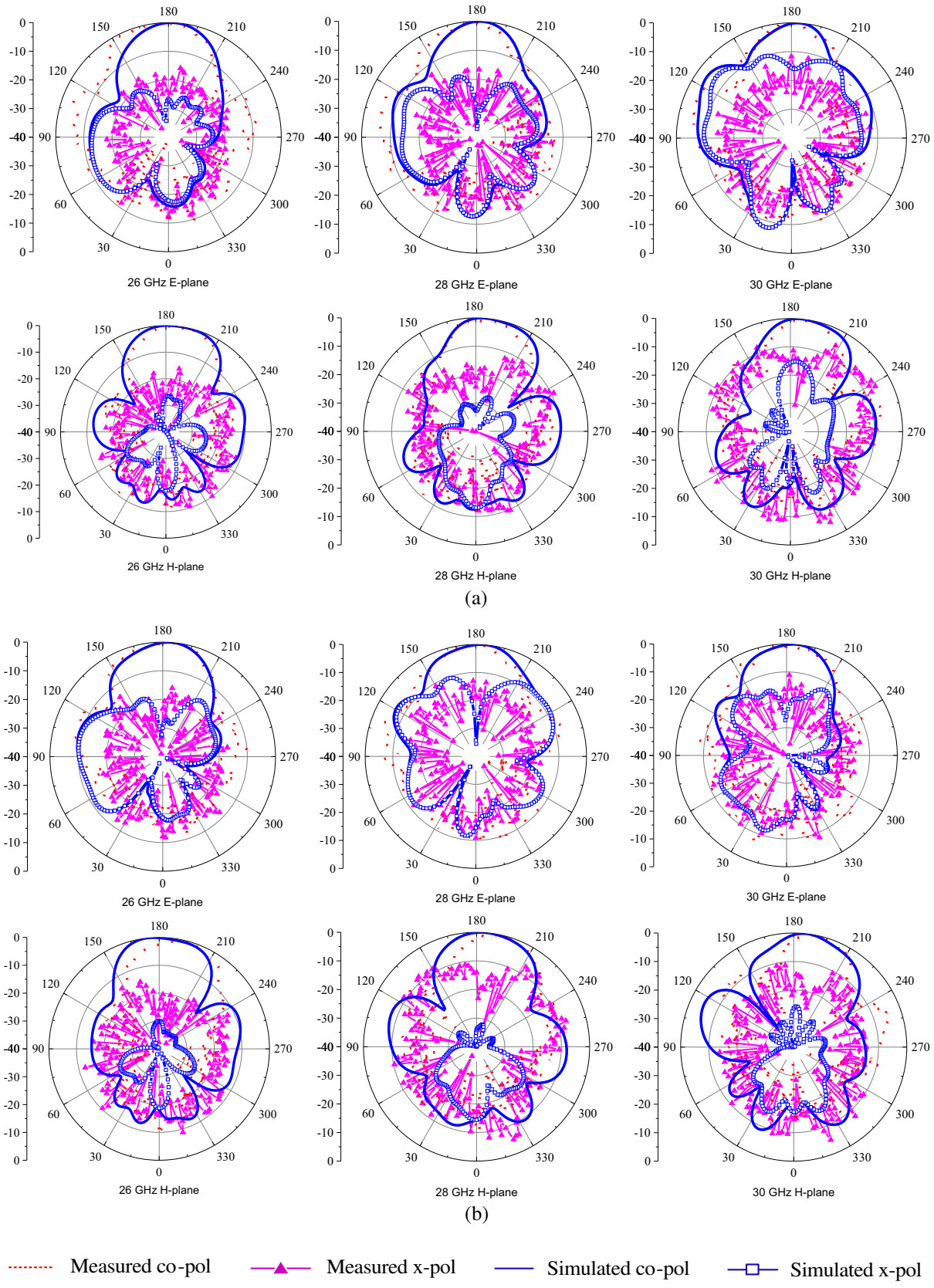

Figure 8. Simulated and measured E-plane and H-plane normalized radiation patterns at 26 GHz, 28 GHz, and 30 GHz. (a) Without via fence. (b) With via fence.

Table 2. Comparisons between the proposed and reported antennas.

Ref.	Method	No. of elements	Max Reduction in $\lvert S_{21}\rvert$ (dB)	Measured Imp. BW (-10 dB) (%)	Measured peak gain (dBi)	Dimension (λ_0^3)	Material
[3]	Metamaterial	2×2	25	3.9	2.3	$0.8 \times 0.8 \times 0.19$	Taconic RF60
[5]	EBG	1×2	15	14.8	7	$1.35 \times 1.14 \times 0.13$	Rogers4003
[14]	Decoupling network	1×2	58	9.2	6.88	$1.01 \times 1 \times 0.2$	-
[18]	Via fence	1×1	32	3	5.6	$0.19 \times 0.19 \times 0.07$	F4BM
This work	Via fence	2×2	37.4	19	9.5	$1.6 \times 1.6 \times 0.2$	FR4

4. CONCLUSIONS

A 2×2 surface-mount dipole antenna array based on via fence for 5G millimeter-wave has been presented. The via fence in the array significantly reduces the coupling between adjacent antenna elements and enhances isolation. The measurement results show that the -10 dB impedance bandwidth is 19%, and the isolation between the adjacent antenna elements is less than -28.76 dB in the range of 24.2–29.5 GHz (N257 (26.5–29.5 GHz), N258 (24.25–27.5 GHz), and N261 (27.5–28.35 GHz)). The compact size, low cost, and high isolation characteristics make the proposed antenna array one of the promising candidates for 5G millimeter-wave applications.

ACKNOWLEDGMENT

The authors would like to thank Prof Hongxing Zheng of the School of Electronics and Information Engineering, Hebei University of Technology, for helping with the antenna measurements.

REFERENCES

1. Andrews, J. G., et al., "What will 5G be?" *IEEE J. Sel. Areas Commun.*, Vol. 32, No. 6, 1065–1082, Jun. 2014, doi: 10.1109/JSAC.2014.2328098.
2. Rappaport, T. S., et al., "Millimeter wave mobile communications for 5G cellular: It will work!," *IEEE Access*, Vol. 1, 335–349, 2013, doi: 10.1109/ACCESS.2013.2260813.
3. Zhang, J., J. Li, and J. Chen, "Mutual coupling reduction of a circularly polarized four-element antenna array using metamaterial absorber for unmanned vehicles," *IEEE Access*, Vol. 7, 57469–57475, 2019, doi: 10.1109/ACCESS.2019.2913552.
4. Luan, H., C. Chen, W. Chen, L. Zhou, H. Zhang, and Z. Zhang, "Mutual coupling reduction of closely E/H-plane coupled antennas through metasurfaces," *IEEE Antennas Wirel. Propag. Lett.*, Vol. 18, No. 10, 1996–2000, Oct. 2019, doi: 10.1109/LAWP.2019.2936096.
5. Shen, X., Y. Liu, L. Zhao, G. Huang, X. Shi, and Q. Huang, "A miniaturized microstrip antenna array at 5G millimeter-wave band," *IEEE Antennas Wirel. Propag. Lett.*, Vol. 18, No. 8, 1671–1675, Aug. 2019, doi: 10.1109/LAWP.2019.2927460.
6. Exposito-Dominguez, G., J.-M. Fernandez-Gonzalez, P. Padilla, and M. Sierra-Castaner, "Mutual coupling reduction using EBG in steering antennas," *IEEE Antennas Wirel. Propag. Lett.*, Vol. 11, 1265–1268, 2012, doi: 10.1109/LAWP.2012.2226013.
7. Abedin, M. F. and M. Ali, "Effects of a smaller unit cell planar EBG structure on the mutual coupling of a printed dipole array," *IEEE Antennas Wirel. Propag. Lett.*, Vol. 4, 274–276, 2005, doi: 10.1109/LAWP.2005.854004.

8. Farahani, H. S., M. Veysi, M. Kamyab, and A. Tadjalli, "Mutual coupling reduction in patch antenna arrays using a UC-EBG superstrate," *IEEE Antennas Wirel. Propag. Lett.*, Vol. 9, 57–59, 2010, doi: 10.1109/LAWP.2010.2042565.
9. Dalal, P. and S. K. Dhull, "Design of triple band-notched UWB MIMO/diversity antenna using triple bandgap EBG structure," *Progress In Electromagnetics Research C*, Vol. 113, 197–209, 2021.
10. Zhang, Y., J.-Y. Deng, M.-J. Li, D. Sun, and L.-X. Guo, "A MIMO dielectric resonator antenna with improved isolation for 5G mm-Wave applications," *IEEE Antennas Wirel. Propag. Lett.*, Vol. 18, No. 4, 747–751, Apr. 2019, doi: 10/ghbsx7.
11. Farsi, S., H. Aliakbarian, D. Schreurs, B. Nauwelaers, and G. A. E. Vandenbosch, "Mutual coupling reduction between planar antennas by using a simple microstrip U-section," *IEEE Antennas Wirel. Propag. Lett.*, Vol. 11, 1501–1503, 2012, doi: 10.1109/LAWP.2012.2232274.
12. Habashi, A., J. Nourinia, and C. Ghobadi, "Mutual coupling reduction between very closely spaced patch antennas using low-profile folded split-ring resonators (FSRRs)," *IEEE Antennas Wirel. Propag. Lett.*, Vol. 10, 862–865, 2011, doi: 10.1109/LAWP.2011.2165931.
13. Vishvaksenan, K. S., K. Mithra, R. Kalaiarasan, and K. S. Raj, "Mutual coupling reduction in microstrip patch antenna arrays using parallel coupled-line resonators," *IEEE Antennas Wirel. Propag. Lett.*, Vol. 16, 2146–2149, 2017, doi: 10.1109/LAWP.2017.2700521.
14. Xia, R.-L., S.-W. Qu, P.-F. Li, Q. Jiang, and Z.-P. Nie, "An efficient decoupling feeding network for microstrip antenna array," *IEEE Antennas Wirel. Propag. Lett.*, Vol. 14, 871–874, 2015, doi: 10.1109/LAWP.2014.2380786.
15. Li, M., M. Wang, L. Jiang, and L. K. Yeung, "Decoupling of antennas with adjacent frequency bands using cascaded decoupling network," *IEEE Trans. Antennas Propag.*, Vol. 69, No. 2, 1173–1178, Feb. 2021, doi: 10/gk6nm5.
16. Zou, X.-J., G.-M. Wang, Y.-W. Wang, and H.-P. Li, "An efficient decoupling network between feeding points for multielement linear arrays," *IEEE Trans. Antennas Propag.*, Vol. 67, No. 5, 3101–3108, May 2019, doi: 10/gk6nm7.
17. Zhang, Y. P., "Enrichment of package antenna approach with dual feeds, guard ring, and fences of vias," *IEEE Trans. Adv. Packag.*, Vol. 32, No. 3, 612–618, Aug. 2009, doi: 10.1109/TADVP.2008.2001769.
18. He, Y. and Y. Li, "Dual-polarized microstrip antennas with capacitive via fence for wide beamwidth and high isolation," *IEEE Trans. Antennas Propag.*, Vol. 68, No. 7, 5095–5103, Jul. 2020, doi: 10/gg9xgv.